THE BELL SYSTEM TECHNICAL JOURNAL
Vol. 57, No. 8, October 1978
*Printed in U.S.A.*

# The Reliability of 302A Numerics

By A. S. JORDAN, R. H. PEAKER, R. H. SAUL, H. J. BRAUN, and H. H. WADE

(Manuscript received December 9, 1977)

*To assess the long-term reliability of Western Electric 7-segment 302A numerics, accelerated forward bias-aging (10 mA, 60° and 125°C) and thermal cycling (−40° to 125°C) experiments have been performed. In treating the bias-aging data, we strictly differentiate between LED chip and digit failure and show that the times to chip failure—defined here as the times required to reach a normalized efficiency of $r = \eta/\eta_0 = 0.5$—are lognormally distributed. The analysis of the data was facilitated by a novel computer-graphics routine which provides for each digit on test a bar-by-bar description of the time-evolution of r. The median life and standard deviation at 125°C and 10 mA for chips are 2400 hours and ~0.4, respectively. Furthermore, we find that the failure distribution for digits can be obtained from the chip distribution by a simple probabilistic consideration. The good accord demonstrated between the experimental data and the theoretical curve derived from the diffusion theory of red GaP LED degradation indicates that the predominant mode of degradation in bias-aging of 302A devices is that of the LED.*

*The thermal cycling response of 302A numerics encapsulated in Hysol 1700 epoxy is excellent. Similar to bias-aging, the chip failure distribution is lognormal, and chip and digit failures are interrelated by the probabilistic law. For a temperature excursion between −40° and 125°C, the median number of cycles to failure is 23,350 for chips and 300 for digits. The cause of failure is identified by electrical testing as open wire bonds.*

*Finally, the acquired data permit the estimation of the mean times to failure (MTTF) and failure rates beyond infant mortality of 302A numerics in a specific application such as Transaction telephone sets under realistic operating conditions. The overall reliability of these devices is excellent, characterized by an MTTF of $10^6$ hours and a maximum failure rate of less than 1 FIT for bias-aging over a 20-year service life. Failures due to broken wires are estimated to yield an MTTF of $10^9$ hours and a failure rate of $\lesssim 4$ FITs at 20 years of service.*

## I. INTRODUCTION

The 302A and 302C red numeric displays designed* by Bell Laboratories and manufactured by Western Electric—Reading consist of 8 red GaP chips arranged as 7 segments into a single digit and a right-hand decimal point. Each chip is mounted in a separate reflector and connected with either a common cathode (302A) or common anode (302C). In both cases, the device is encapsulated in Hysol 1700 epoxy.†

In general, the effects of long-term thermomechanical, environmental, and electrical operating conditions on device performance are determined concurrently with device development. The major objective of this work was to obtain reliability information on 302A numeric display devices by means of forward bias-aging and thermal cycling at accelerated rates, which enables us to predict their long-term behavior, beyond infant mortality, when used in typical Bell System applications.

First, we provide an outline of the experimental procedures employed in the acquisition of failure data by high temperature forward bias-aging and wide temperature-range thermal cycling. Then, the handling, treatment, and graphic display of the copious amount of information generated by the bias-aging experiments are discussed. Second, the time evolution of the relative luminescent efficiency ($r = \eta_t/\eta_0$) of 302A numerics during bias-aging is compared to the predictions of the diffusion theory of red GaP degradation.[1] Moreover, the failure distribution is established for the entire sample of chips. Next, we determine the failure distribution for thermal cycling and attempt to locate the thermomechanical weak points of a bonded chip. Finally, we discuss the evaluation of the mean time to failure (MTTF) by a variety of criteria (i.e., alternative definitions of chip and digit failure). It is shown on the basis of probabilistic arguments that the failure distribution for digits can be calculated from the chip distribution. Likewise, in the case of thermal cycling, chip and digit distributions are convertible. The parametric values under normal operating conditions can be extrapolated from accelerated failure data by means of semi-empirical correlations. When they are combined with a device utilization model for a specific application, the MTTFs and failure rates induced by the forward bias and temperature cycling can be readily estimated.

## II. EXPERIMENTAL

### *2.1 Bias-aging*

Seventeen 302A numeric devices were selected for long-term elevated temperature forward bias-aging. Prior to aging (at $t = 0$), the light output of every segment was measured at 25°C by a standard technique.[2]

* The device was designed by C. R. Paola.
† A product of the Hysol Division, Dexter Corporation.

Briefly, the output was determined segment by segment over a wide range of pulsed test current inputs between 1 and 100 mA (including 2, 5, 10, 20, and 50 mA). At each pulsed current, the duty cycle was adjusted to assure a constant 1 mA dc average current to minimize junction heating. The segment electroluminescence was detected by a PIN 10 diode and its output after amplification was handled by an appropriate software program on an HP 9830A minicomputer to yield a table of information stored on a computer file for all devices under testing.* The table contains the light output of each segment of a given device measured over the entire range of measuring currents employed. The lowest and average initial light outputs were 0.021 and 0.035 millicandella/mA, respectively.

Following initial testing, the 17 devices were split into two groups (9 and 8 units in each group). One of the groups was aged at 60°, the other one at 125°C, in ovens continuously purged with filtered $N_2$. The devices were placed in trays, each holding three devices, connected to power supplies providing 10 mA dc forward bias. Periodically, all the devices were removed from the ovens to determine the effect of bias-aging on light output. Before performing the measurements by the above-described procedure, the devices were allowed to cool for two hours to 25°C.

### *2.2 Thermal cycling*

Ten 302A numerics were subjected to continuous temperature cycling without bias in a controlled-environment chamber. Each cycle consisted of cooling the devices in the chamber from room temperature (~25°C) to a cold dwelling point at −40°C, then reversing to a warm dwelling point at 125°C, and finally returning to ~25°C. At each temperature extreme, the dwelling time was about 20 minutes. The cooling and heating rates never exceeded 5°C/min.

The devices were mounted in ceramic sockets attached to a combination aluminum and phenolic test fixture through which electrical connections could be made for periodic checks. As a result of progressive thermal cycling, dark segments could be visually observed at the standard forward current of 10 mA dc. All the defective chips were faulty at both temperature extremes as well as at room temperature. For the duration of the first 100 cycles, checks were made at about every 5 cycles; thereafter, the test interval was increased to approximately 25 cycles.

* The automated test facility was developed by J. W. Mann.

## III. DATA HANDLING PROCEDURE

Whenever the degraded light output is measured, each device in the sample is characterized by 8 segments × 8 electrical values (including the decimal point and the device voltage at 10 mA). For a total sample of 17 devices, as many as 1088 numbers are acquired per test at all current levels. Obviously, computer storage, retrieval, and treatment of the data together with a suitable graphic display are required for detailed analysis. Therefore, a time-sharing program has been developed which plots the relative electroluminescent efficiency in a unique manner. First, the program LED/EFFCAL reads the permanently stored file of raw data generated by each light output measurement of any $t$. A short terminal dialog permits the user to name the type of device involved because, in addition to the 302A, the program is also applicable to other classes of numerics as well as to a group of 10 discrete LED chips. Moreover, one can specify the aging temperature and room temperature test current and one of the two plotting scales. Then, a file is written which includes the device identification number, aging temperature, total accumulated aging time, test current, and the number of devices in test under listed conditions. Moreover, an array is created from the raw data which, for every digit of each device,* contains, segment by segment, the relative efficiency as a function of the elapsed aging time.

As shown in Fig. 1, in accord with the accepted convention, the segments are designated by the alphabetic codes $A, B \ldots G$. For the $A$ segment of the $i$th device, the relative efficiency at $t$ is given by

$$r_A^i = \frac{\eta_A^i(t)}{\eta_A^i(0)}, \tag{1}$$

where the conversion factor relating light output to electroluminescent efficiency $\eta$ was cancelled. The array includes $r_A^i$ for each time the light output has been measured. In addition, it may be interesting to know the relative degradation of any segment in comparison with the mean value. For this reason, we devised the following statistical indicators:

($i$) Device or digit mean, $\bar{r}_i$

$$\bar{r}_i = \frac{\sum_{A=1}^{7} r_A^i}{7}. \tag{2}$$

($ii$) Grand mean, $\bar{r}$

$$\bar{r} = \frac{\sum_{i=1}^{n}\sum_{A=1}^{7} r_A^i}{7n} = \frac{\sum_{i=1}^{n} \bar{r}_i}{n}, \tag{3}$$

where $n$ is the number of devices tested under identical conditions.

* Although in the case of a 302A numeric each device corresponds to a digit, allowance is made in the program for numerics which consist of as many as 4 digits per device.

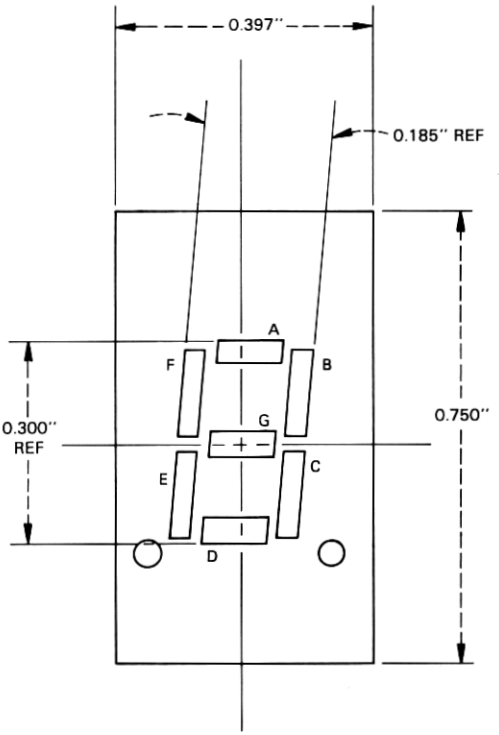


Fig. 1—Top view of a 302A device showing letter designation of segments.

(*iii*) Standard deviation—upper and lower confidence limits of the grand mean at ~68-percent confidence level, $\bar{r}_u$ and $\bar{r}_\ell$

$$\bar{r}_u = \bar{r} + \frac{\left(\sum_{i=1}^{n}\sum_{A=1}^{7}(r_A^i - \bar{r})^2\right)^{1/2}}{7n} \tag{4a}$$

and

$$\bar{r}_\ell = \bar{r} - \frac{\left(\sum_{i=1}^{n}\sum_{A=1}^{7}(r_A^i - \bar{r})^2\right)^{1/2}}{7n}. \tag{4b}$$

At the beginning of the file written for a given set of test conditions (i.e., aging temperature and current) $\bar{r}$, $\bar{r}_u$ and $\bar{r}_\ell$ are listed in a time sequence. At the end of the file, we find $\bar{r}_i$ as a function of time for each digit.

A batch program named LED/EFFPLT accepts these arrays to produce hard-copy plots of $r$ versus time either using the rapid output STARE 3 system or the FR80 microfilm plotter, especially suitable for white prints or viewgraphs. The two options for scales are $\log_{10} r$ versus square-root of time and $r$ versus $\log_{10}$time. In Fig. 2, a computer-generated graphic

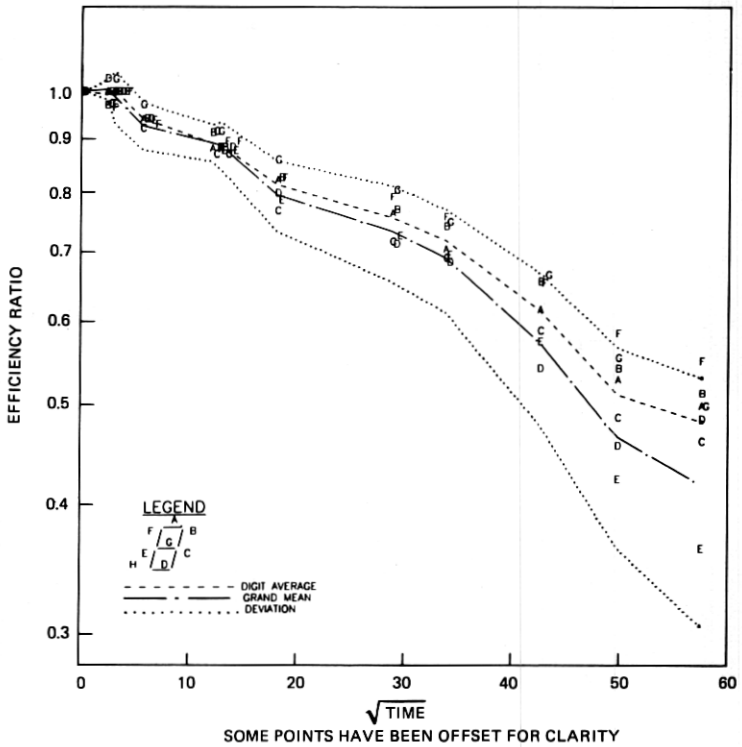


Fig. 2—Computer-generated plot of $\log_{10}$ normalized efficiency ($r = \eta/\eta_0$) versus time $^{1/2}$ [hours$^{1/2}$] for a 302A device aged at 125 °C and 10 mA. The dashed, dash-dot, and dot-dot lines are the digit mean [eq. (2)], grand mean [eq. (3)], and standard deviation of grand mean [eq. (4)], respectively.

output is presented for a 302A device aged at 125°C and 10 mA dc and measured at 10 mA in the $\log_{10} r$ versus $\sqrt{t}$ projection. Note that, for each segment of the digit, the symbol is its alphabetic designation in the order shown in Fig. 1. When overlap of the letters interferes with clarity, a slight horizontal displacement of the symbol along the time axis has been introduced into the plotting routine. In addition to the discrete $r$ values of the individual bars, we also display the device mean, grand mean, and its lower and upper confidence limits by continuous dashed, dash-dot, and dot-dot lines, respectively. In Fig. 3, the data for the same device are presented using the $r$ versus log $t$ scale option. It can be readily seen that, at the chosen testing intervals, the former scale provides an evenly spread distribution of points at long aging times, while the latter ($r$ vs. log $t$) achieves well-separated spacings at short times. Up to 3200 hours, the normalized efficiency of the 302A is apparently independent of time when bias-aged at 60°C. This is shown in Fig. 4 on a $\log_{10} r$ versus $\sqrt{t}$ plot. Although the $r$ scale is magnified here compared to Fig. 2, it does not appear to illustrate more than measurement fluctuations. Of course, this

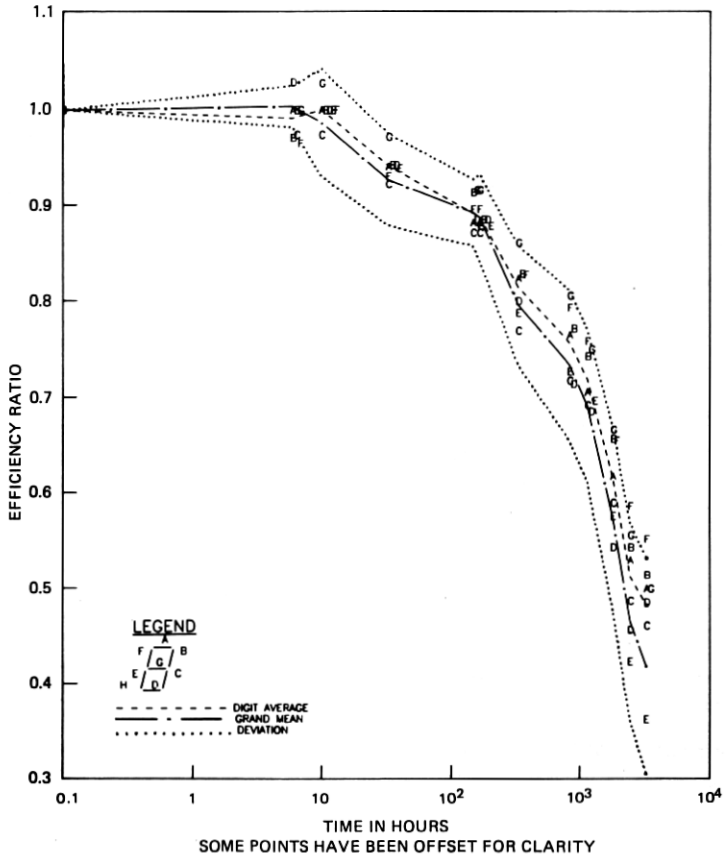


Fig. 3—Computer-generated plot of normalized efficiency ($r = \eta/\eta_0$) versus $\log_{10}$ time for a 302A device aged at 125°C and 10 mA. The dashed, dash-dot, and dot-dot lines are the digit mean [eq. (2)], grand mean [eq. (3)], and standard deviation of grand mean [eq. (4)], respectively.

is consistent with the activation energy of red GaP LED degradation (0.7 eV)[5] which leads to very little change in $r$ at 60°C in the first few thousand hours.

These detailed computer-generated figures are very handy in a rapid assessment of numeric degradation and also as an intermediate step for further analysis. In particular, one can immediately see to what extent an individual chip departs from the digit and grand means. In addition, as shown in the next section, the MTTF of the failure distribution can be readily evaluated from the plots under a variety of failure definitions.

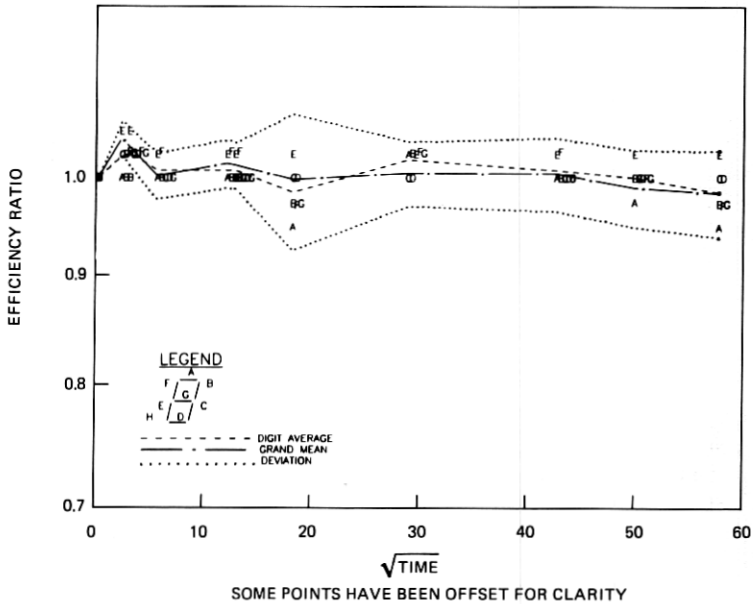


Fig. 4—Computer-generated plot of $\log_{10}$ normalized efficiency ($r = \eta/\eta_0$) versus time$^{1/2}$ [hours]$^{1/2}$ for a 302A device aged at 60°C and 10 mA. The dashed, dash-dot, and dot-dot lines are the digit mean [eq. (2)], grand mean [eq. (3)], and standard deviation of grand mean [eq. (4)], respectively.

## IV. RESULTS AND DISCUSSION

### *4.1 Bias aging*

To compare the bias-aging results on 302A numerics with existing information involving discrete red GaP LED chips, we have replotted from Fig. 3 the grand mean of the normalized efficiency and its standard deviation as a function of $\log_{10}t$ in Fig. 5. Superimposed on the same figure is the calculated course of degradation at 125°C ambient temperature and 10 mA stress current (132°C junction temperature). The theoretical curve is based on the diffusion theory of red GaP LED degradation.[1]

Recently, the time evolution of nonradiative centers, thought to be responsible for the long-term degradation of red GaP LEDs, has been modeled. It has been postulated that degradation is due to the diffusion and accumulation of an undesirable impurity or point defect through the depletion layer as the p-n junction potential, which retards defect motion, is reduced by the forward voltage. An explicit analytical expression between $r$ and $t$ was derived which provided a good fit to the degradation data for discrete diodes obtained at various junction temperatures and stress currents. The equation for $r$ is of the form[1]

$$r(t) = \frac{1}{\sqrt{1 + r_0 + \gamma\varphi(t/\theta)}}, \tag{5a}$$

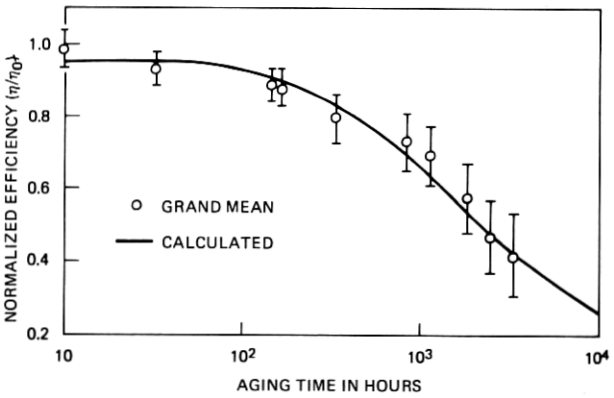


Fig. 5—Normalized efficiency versus $\log_{10}$ time for 302A numerics aged at 125°C and 10 mA. The full line is calculated from the diffusion theory of red LED degradation [eq. (5)]. The data points are the grand mean and its standard deviation for all segments of the sample (see Fig. 3).

where $\varphi$ is an infinite series, $\gamma$ is a constant which is proportional (among other quantities) to the initial undesirable impurity concentration and electron lifetime of a diode lot, and $r_0$ reflects the rapid drop in $\eta$ at relatively short aging times. The quantity $\theta$ is related to the diffusivity ($D_0$), activation energy ($\Delta H_a$), and stress current ($I_{\text{stress}}$) according to

$$\frac{1}{\theta} = \alpha I_{\text{stress}} e^{-\Delta H_a/kT}, \tag{5b}$$

where $\alpha$ is a known constant of proportionality.

To calculate the degradation curve in Fig. 5 from eqs. (5), we made use of the parameters listed in Ref. 1. However, on account of the lot-dependent properties of $\gamma$, a small upward adjustment in its value was required to achieve optimum description of the data. Without this change, the computed $r$ values would be approximately 10 percent above the plotted ones at times in excess of 1000 hours.

The good agreement seen between the experimental normalized efficiencies for 302A numerics and the theoretical curve indicates that these red devices do not exhibit failure modes in addition to LED degradation. This finding is corroborated by the 125°C storage aging of numerics which has not discolored the Hysol 1700 encapsulant. Thus, it appears that the optical coupling efficiency of 302A numerics is invariant during bias aging.

Since the normalized efficiency of individual segments visibly deviates from the grand mean (Fig. 2), the failure of 302A numerics must be distributed by some statistical law. Detailed digit-by-digit failure plots similar to Fig. 2 permit the determination of the failure distribution as a consequence of bias aging. The following possible failure criteria are worthy of exposition in some detail:

(*i*) Chip failure: Whenever any one of the $7n$ chips in the samples reaches $r_A^i = 0.5$, that time is denoted as the time to chip failure (TTCF).

(*ii*) Digit failure: The time for the first chip in each device to attain $r_A^i = 0.5$ is designated as the time to digit failure (TTDF).

(*iii*) Digit mean failure: The time for any digit mean $\bar{r}_i$ [eq. (2)] to equal 0.5 is named the time to digit mean failure (TTDMF);

(*iv*) Grand mean failure: When the grand mean normalized efficiency [eq. (3)] $\bar{r} = 0.5$, we speak of time to grand mean failure (TTGMF). Each one of these quantities possesses a mean except TTGMF.

The total number of chips in our sample of 8 aged at 125°C is $8 \times 7 = 56$. In Fig. 6, we present on lognormal graph paper the time to chip failure as a function of cumulative failure percent.[3,4] The TTCF values were taken from computer-generated plots for each 302A digit, identical in form with Fig. 2, and then rank-ordered to provide the cumulative failure. It should be noted that TTCFs above ~3400 hours were obtained by linear extrapolation on the $\sqrt{t}$ plots.[5] Hence, the longer the time to chip failure is, the less accurate the TTCF value becomes. Fortunately, this is probably not important except in the case of the last two points.

The linearity of the TTCF plot in Fig. 6 indicates that the failure distribution for 302A numeric chips is lognormal, as is the case for 1A opto-isolators,[6] which utilize GaP LEDs and also for numerous semiconductor devices.[7] Least-square analysis provides the following lognormal parameters for the chip failure distribution.[4]

$$\mu_a = \ln t_{ma} = 7.783$$
$$\sigma_a = 0.37,$$

where the median life, $t_{ma}$, is 2400 hours. It can be seen that the distribution is very tight, as $\sigma_a$ is quite small.

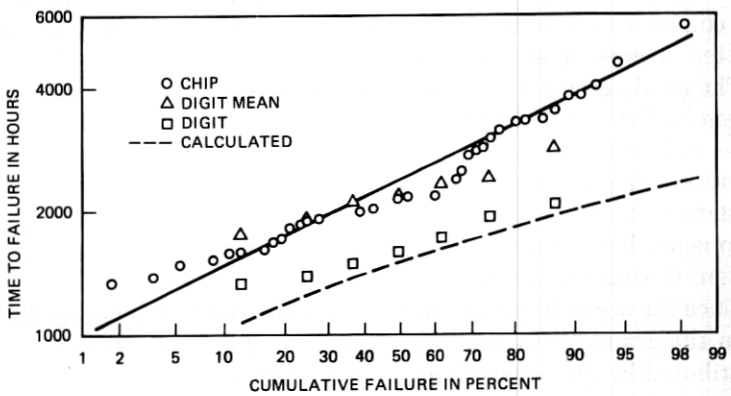


Fig. 6—Time to failure versus cumulative failure percent for 302A numerics aged at 125°C and 10 mA. The symbols O, □, and Δ correspond to failure criteria (*i*), (*ii*), and (*iii*), respectively (see text). The solid line is a least-square line for chip failure, while the dashed line is calculated from eq. (9) for digit failures.

The time to digit mean failure as a function of cumulative failure percent is also shown in Fig. 6. Each one of the computer-generated plots for each device, similar to Fig. 2, yields one value of TTDMF. Because each time value is the result of averaging seven normalized efficiencies, the standard variation is smaller than for TTCF. However, the median life $t_{mc}$ = 2200 hours, which is almost the same as for chip failure.

Perhaps the most important distribution for numerics is the time to digit failure, since it is reasonable to assume that if any one chip in a 7-bar numeric loses half its efficiency, the displayed numerals may not be correctly discriminated by eye. The TTDF distribution is also shown in Fig. 6. Its construction from the computer-generated digit-by-digit graphic outputs is self-evident. We can see that in comparison with a $t_{ma}$ of 2400 hours for chips, the median life for digits, $t_{mb}$, is reduced to 1600 hours with an accompanying decrease in $\sigma$. In Table I, we summarize the median lives obtained by a variety of methods. It can be seen that all the values but the median of TTDF are closely spaced.

However, the chip and digit failure distributions are related by the laws of probability. The reliability function for chip failure $R_a$ is the complement of the plotted cumulative failure $Q_a$, hence at any time $t$

$$R_a(t) = 1 - Q_a(t). \tag{6}$$

$R_a$ expresses the probability that the chip will survive to $t$. If the chip failures in the device are independent, then the reliability of the digit, $R_b$, assuming device failure if any one of the segments fails ($r_A^i \leq 0.5$), is given by[8]

$$R_b(t) = R_a^7(t). \tag{7}$$

Obviously, the TTDF definition is consistent with eq. (7). The cumulative failure function for device failure, $Q_b$, is of the form

$$Q_b(t) = 1 - R_b(t) = 1 - R_a^7(t). \tag{8}$$

Finally, a combination of eqs. (6) and (8) yields

$$Q_b(t) = 1 - (1 - Q_a(t))^7. \tag{9}$$

The cumulative device failure function $Q_b$ for 302A numerics can be

Table I — Median lives for a 302A red numeric at 125°C and 10 mA

| Method | $t_m$ (hours) |
|---|---|
| Chip failure | 2400 |
| Digit mean failure | 2200 |
| Digit failure | 1600 |
| Grand mean failure* | 2300 |
| Diffusion theory ($r$ = 0.5)* | 2200 |

* Not a median but a single value.

readily obtained from the full line (lognormal distribution) in Fig. 6 and eq. (9). The dashed line in Fig. 6 is the calculated $Q_b$. Considering the small sample size in terms of digits, the calculated line is a surprisingly good representation of the cumulative failure data for digits. The median life appropriate for $Q_b$ is 1500 hours, which should be compared with the empirical result of 1600 hours. Therefore, it matters very little how the median lives are computed (chip versus device), as long as the results are correctly interpreted. Furthermore, although the median lives obtained by various criteria nearly coalesce, this may not be true of the MTTFs and failure rates as those quantities also involve the standard deviations which, according to the slopes over the data in Fig. 6, are quite variable.

### *4.2 Thermal cycling*

In thermal cycling, chip failure is sudden and manifests itself as a dark segment on testing. In analogy with the definition invoked in the section on bias-aging, digit failure occurs at the number of thermal cycles at which the very first segment fails to light up. In Fig. 7, we present a lognormal projection of the number of cycles to failure versus cumulative failure percent, both in terms of chip as well as device failure, for 302A red numerics encapsulated in Hysol 1700 epoxy.

Again, as in the case of bias-aging, the failure distribution follows the lognormal pattern, as it plots as a straight line on the lognormal graph-paper. Least-square analysis yields the following parameters for chip failure:

$$\mu_{tc} = \ln t_{mtc} = 10 \text{ and } \sigma_{tc} = 3.27,$$

where $t_{mtc} = 23{,}350$ is the median number of cycles to failure (MCTF). The large standard deviation corresponds to a widely spread failure distribution. This is also clear from the steepness of the data and the least-square (solid) line in Fig. 7.

The probabilistic equation derived in the previous section on bias-aging to calculate the digit failure distribution from information on chips is also valid for thermal cycling. Applying eq. (9) to the lognormal line for chips, we can calculate the number of thermal cycles to failure as a function of cumulative failure function for digits. The dashed line in Fig. 7 represents the digit cumulative failure function. The digit MCTF is 300. It is apparent that there is excellent agreement between the theoretical line and the data points for digit failure.

The effect of increasing the number of digits in the same package is also shown in Fig. 7. The dash-dot line is the cumulative failure function for a hypothetical 302A-like device consisting of four digits (28 bars). It is obvious that, with increasing complexity, there is a drastic drop in the MCTF with a somewhat compensating drop in standard deviation.

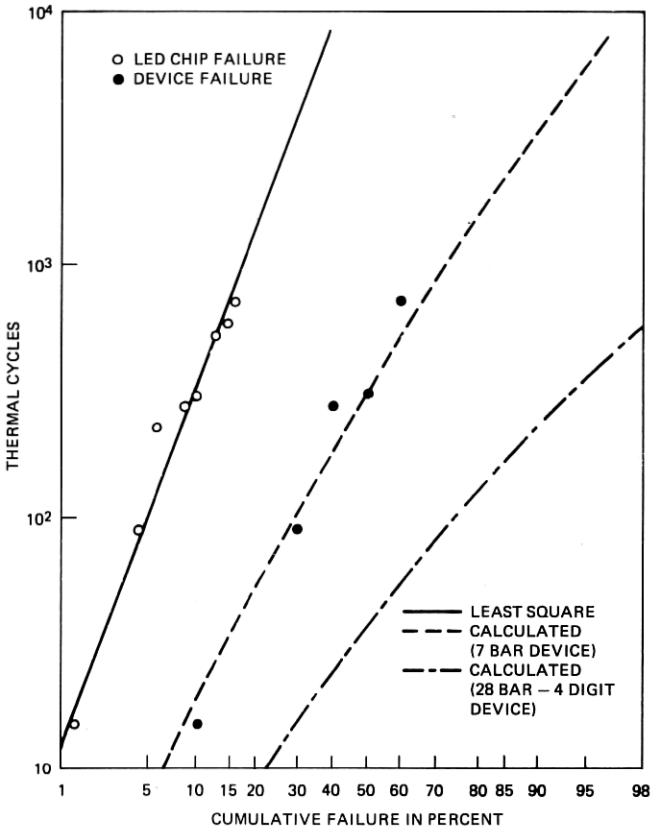


Fig. 7—Number of thermal cycles to failure versus cumulative failure percent for 302A numerics, encapsulated in Hysol 1700 epoxy, thermally cycled between −40° and 125°C. The solid line is a least-square line for chip failure, while the dashed line is calculated from eq. (9) for digit failure.

To locate the source of thermal cycle failure, a number of devices with numerous chip failures were lapped and polished until the gold leads to the diodes were exposed. A detailed view of the lapped area of a 302A numeric is illustrated in Fig. 8. The polishing of the lens continued to the point at which the anode connecting Au wire was broken between the lead frame and the die-bonding pad. Due to the ambiguity of viewing the location of failure, simple electrical checks were performed. Using cathode pins as the common terminal, a fine needle point probe with +2V bias was successively applied to the ends of the severed Au wire and to the bonding pads by piercing the plastic. As a result of such tests, we determined that, after thermal cycling, open circuits develop which are evenly distributed between breaks in the neck of the ball bond and the heel of the wedge bond.

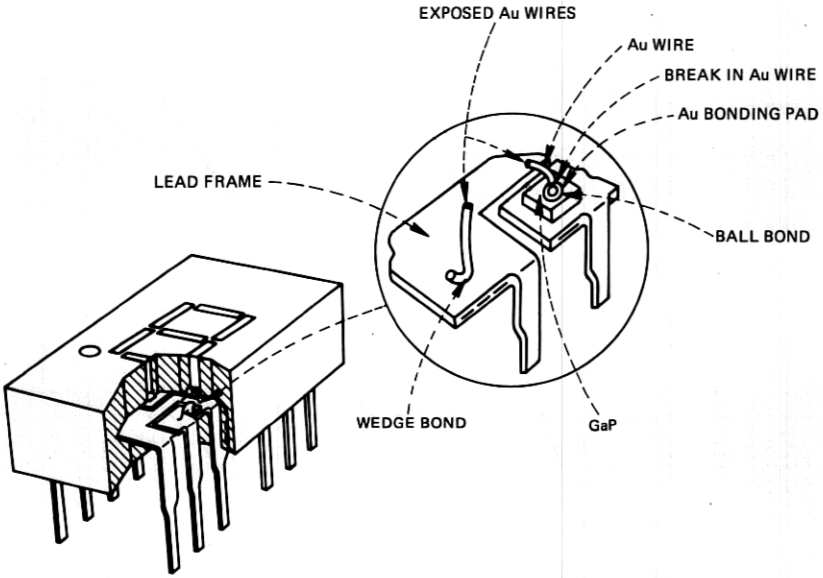


Fig. 8—Cutaway view of a 302A numeric showing the exposed bonds.

### *4.3 Reliability calculations—device utilization model*

It should be very strongly emphasized that the adequacy of a given median life and $\sigma$ combination based on exhaustive tests can only be judged if the device designer possesses information from systems engineering on its anticipated application. Hence, a device utilization model for the 302A numeric is essential.

One use of the 302A display is in Transaction telephone sets. If we envision very frequent operation, such as in airline terminals, fresh information may appear on the displays as often as every minute for a 30-s duration. The devices operate at 10 mA dc, which leads to a 7°C junction heating. Thus, if the ambient temperature is 27°C, the devices are exposed to 34°C. During the off-state, the time (30 s) is too short to reach thermal equilibrium with the ambient. Therefore, we assume a temperature fluctuation or cycling excursion of no more than $\Delta T$ = 2°C.

The model in combination with the reliability data derived herein permit the estimation of the failure rates and MTTFs during device operation under forward bias, and also on account of temperature variations. We shall give the reliability-associated properties for both LED chips and digits at 20 years of service.

(*i*) Bias Aging: The accepted activation energy for red LED degradation is 0.7 eV.[5] With this value, the Arrhenius-law multiplier between the aging temperature (132°C) and use temperature (34°C) becomes 604. Applying the multiplier to the chip and digit median lives, $t_{ma}$ = 2400

and $t_{mb}$ = 1600 hours, respectively, we obtain at the use temperature*

$$t_{ma}(34°\text{C}) = 1.45 \times 10^6 \text{ hours}, \; t_{mb} = 9.66 \times 10^5 \text{ hours}.$$

The standard deviations are usually taken as temperature-independent constants, and their values are

$$\sigma_a = 0.37 \text{ and } \sigma_b = 0.27.$$

It should be noted that the device failure distribution ($Q_b$) is not strictly lognormal and $\sigma_b$ results from the linearization of the dashed line in Fig. 6.

The above parameters yield the following MTTFs† and maximum failure rates for a 20-year‡ service life beyond infant mortality:[3,4]

$$\text{MTTF}_a = 1.57 \times 10^6 \text{ hours and } \text{MTTF}_b = 1.01 \times 10^6 \text{ hours}$$

and

$$\lambda_a \ll 1 \text{ FIT and } \lambda_b \ll 1 \text{ FIT}.$$

These failure rates for bias aging are outstandingly low. This is a consequence of the fact that both the chip and device distributions, as shown in Fig. 6, are very tight, corresponding to a small $\sigma$. If it is assumed that the investigated lot was atypical and occasionally $\sigma_a$ and $\sigma_b$ may become as large as 1 and 0.9, respectively, then we obtain for the $\lambda$s

$$\lambda_a = 90 \text{ FITs and } \lambda_b = 150 \text{ FITs},$$

indicating, as expected, that the failure rate for chips is less than for digits.

(*ii*) Thermal Cycling: To relate the median number of cycles to failure, MCTF, obtained by long-term wide $\Delta T$ excursion experiments to the small $\Delta T$ excursions encountered in use, an acceleration factor is required. We have estimated this factor on the basis of previous work on gold beam fatigue. Dais and Howland[9] have shown, for rubber encapsulated devices tested in the plastic deformation domain, that the magnitude of the temperature excursion between $\Delta T$ = 400° and 45°C is a monotonically decreasing function of the median number of cycles to failure. We can characterize the dependence of $\Delta T$ on cycles by a power law with an exponent increasing from $\sim -0.5$ (Coffin's Law[10]) to a limiting value of $\sim -0.1$. In addition, theoretical analysis of typical device structures indicates that the magnitude of the maximum elastic $\Delta T$ span for rubber encapsulant is about twice that for epoxy.[11] Thus,

---

* The subscripts $a$ and $b$ denote chip and device reliability properties, in accordance with the definitions in Section 4.1.

† MTTF = $t_m e^{\sigma^2/2}$.

‡ The effective service life is only 10 years due to the duty factor of 0.5.

it seems reasonable to take $\Delta T = 20°C$ as the transition temperature between elastic and plastic deformation for the epoxy encapsulant. Consequently, by extrapolating the results of Dais and Howland[9] between $\Delta T = 165°$ and 20°C, we obtain $\sim 3 \times 10^7$ as the approximate acceleration factor appropriate for 302A numerics. Since a temperature cycling range of only 2°C is anticipated in use, the deformation always remains elastic. Hence, the acceleration factor and failure rates given here should be considered as lower and upper bounds, respectively.

A combination of the acceleration factor and the experimental values $\text{MCTF}_{expa}$ (23350) and $\text{MCTF}_{expb}$ (300 cycles) for chip ($a$) and digit ($b$) failure, respectively, yields

$$\text{MCTF}_{usea} = 7 \times 10^{11} \text{ cycles and } \text{MCTF}_{useb} = 9 \times 10^9 \text{ cycles}$$

$$\text{and } \sigma_{tca} = 3.27 \text{ and } \sigma_{tcb} = 2,$$

where $\sigma_{tcb}$ is from the hypothetical linearization of the dashed line in Fig. 7. Since in operation there are 60 cycles/hour, the median lives become

$$t_{mtca} = 1.2 \times 10^{10} \text{ hours and } t_{mtcb} = 1.5 \times 10^8 \text{ hours.}$$

The above parameters yield the following MTTFs and failure rates, $\lambda_{tc}$, at 20 years of service life:[3,4]

$$\text{MTTF}_{tca} = 2.5 \times 10^{12} \text{ hours and } \text{MTTF}_{tcb} = 1.1 \times 10^9 \text{ hours}$$

$$\lambda_{tca} = 2 \text{ FITS and } \lambda_{tcb} = 4 \text{ FITs.}$$

In conclusion, we find that the 302A red numeric performs very reliably in specific applications such as the Transaction telephone. We have shown that the long-term failure rates associated with LED degradation and junction heating induced thermal cycling are very low, namely, no more than 4 FITs over 20 years of continuous service.

## V. ACKNOWLEDGMENTS

We are grateful to G. A. Dodson for a critical review of the manuscript. We appreciate the useful practical advice provided by C. R. Paola, B. Johnson, and J. W. Mann.

## REFERENCES

1. A. S. Jordan and J. M. Ralston, J. Appl. Phys., *47* (1976), p. 4518.
2. J. M. Ralston, Rev. Scientific Instruments, *43* (1972), p. 876.
3. J. Aitchison and J. A. C. Brown, "The Lognormal Distribution," Cambridge: Cambridge University Press, 1957.
4. A. S. Jordan, Microelectronics and Reliability, *18*, No. 3 (1978), in press.
5. J. M. Ralston, unpublished work.
6. R. H. Saul, E. H. Nicollian, and D. A. Harrison, unpublished work.

7. D. S. Peck and C. H. Zierdt, Jr., Proc. IEEE, *62* (1974), p. 185.
8. "Reliability Engineering," ARINC Research Corporation, W. H. VonAlven, editor, Englewood Cliffs, N.J.: Prentice-Hall, 1965.
9. J. L. Dais and F. L. Howland, unpublished work.
10. S. S. Manson, "Thermal Stress and Low Cycle Fatigue," New York: McGraw-Hill, 1966.
11. J. L. Dais, unpublished work.